DOE/ET-53088-355 IFSR #355

Self-consistent Radial Sheath

R.D. HAZELTINE

Institute for Fusion Studies and Department of Physics
The University of Texas at Austin
Austin, Texas 78712

December 1988

Self-consistent Radial Sheath

R. D. Hazeltine
Institute for Fusion Studies and Department of Physics
University of Texas at Austin
Austin, Texas 78712

Abstract

The boundary layer arising in the radial vicinity of a tokamak limiter is examined, with special reference to the TEXT tokamak [Nucl. Fusion **27**, 1125 (1987); Phys. Fluids **27**, 2956 (1984)]. It is shown that sheath structure depends upon the self-consistent effects of ion guiding-center orbit modification, as well as the radial variation of $E \times B$-induced toroidal rotation. Reasonable agreement with experiment is obtained from an idealized model which, however simplified, preserves such self-consistent effects. It is argued that the radial sheath, which occurs whenever confining magnetic field-lines lie in the plasma boundary surface, is an object of some intrinsic interest. It differs from the more familiar axial sheath because magnetized charges respond very differently to parallel and perpendicular electric fields.

I. Introduction

The edge of an unmagnetized, bounded plasma exhibits a thin layer in which the plasma density abruptly decays. Strong steady-state electrostatic fields, oriented to confine the faster plasma species, characterize this "Debye sheath," whose width is measured by the Debye length, λ_D.[1] Essentially the same structure develops near the edge of a magnetized plasma, provided that the magnetic field direction is normal to the bounding surface—as occurs, for example, at the end-plate of a magnetic mirror device. In either case the motion of charged particles to or from the bounding wall is constrained by both self-consistent electric field and collisions. We refer to this sheath as an "axial" sheath, since the plasma parameters and fields vary along the direction of the confining field.

However, a magnetized plasma also allows for a fundamentally different sheath structure, which we shall call the "radial" sheath. A radial sheath is formed when magnetic field lines lie in the plane of the plasma boundary, rather than normal to it. It is clear that the mechanisms for self-consistent equilibration are sharply different in this geometry, since particle motion normal to the boundary becomes severely constrained. Such motion occurs either through Larmor gyration, or through guiding-center drifts; in either case the orbits are restricted and only indirectly responsive to sheath electric fields.

We study a specific radial sheath, on which there is considerable experimental data: the limiter scrape-off layer in the TEXT tokamak.[2,3] This sheath is marked by a steep peak in the electrostatic potential, ϕ, roughly centered at $r = a$, where r is the minor radius and a the limiter radius. Typically it is found that $e\phi$ changes by a few times the electron temperature, T_e, over a radial distance of a centimeter or two:

$$\frac{e\phi}{T_e} \sim 3\text{–}5, \quad \left|\frac{d\ln\phi}{dr}\right|^{-1} \sim \text{ 1–2 cm.} \tag{1}$$

This peak in ϕ evidently corresponds to a localized excess of positive charge: a halo of ions surrounding the quasineutral plasma. (It should be emphasized here that the observed potential fluctuates widely, at a frequency near the diamagnetic drift frequency, ω_*; our present comments and subsequent analysis pertain to the steady-state or time-averaged potential.)

TEXT has a single, poloidally symmetric limiter ring. Measurement of the sheath potential (by Langmuir probes as well as ion beam techniques) is effected at a toroidal location diametrically opposite the limiter, some three meters away. Thus, while the limiter is surrounded by the usual (axial) Debye sheath of width λ_D, the potential measurements refer specifically to a radial sheath. It is convenient here to point out that, because of the rapid streaming of electrons along $\mathbf{B}$, the edge region outside of the Debye sheath is effectively axisymmetric.

The origin of excess positive charge near and beyond the limiter radius

has been understood for some time: it is an artifact of the relatively wide radial excursions of ion guiding centers. We recall that the guiding center orbits of charged particles in tokamaks have a radial width measured by their gyroradii in the poloidal field,

$$\rho_p \equiv \left(\frac{B}{B_p}\right)\rho, \tag{2}$$

where ρ is the usual (thermal) gyroradius, B is the total field magnitude and B_p is its poloidal component. For comparable species temperatures, the ion excursion is evidently larger than the electron excursion by $(m_i/m_e)^{1/2}$. For this reason, and also because of the related disparity in parallel streaming speeds, the "halo" region outside the limiter radius is a relative loss region for electrons. Ions, especially those magnetically trapped ions that have the widest orbits, can protrude into the halo while evading the limiter; electrons whose guiding center orbits lie outside the limiter radius are promptly lost.

These remarks lead to a straightforward estimate of the magnitude of the halo charge density:

$$n_i - n_e \sim \frac{\Delta_i^2 d^2 n}{dr^2},$$

where Δ_i is the radial ion orbit width. But the conventional assumption,

$$\Delta_i \sim \rho_{pi} \tag{3}$$

(here aspect-ratio factors—not far from unity—are omitted for simplicity) is found to yield a charge density bigger, by orders of magnitude, than what is observed.

One reason for this disparity is immediately clear. While numerous complications related to ionization, secondary emission and similar effects have been neglected (see below), the estimate is fundamentally inconsistent in its use of Eq. (3). In fact, as can be seen from early work of Berk and Galeev,[4] and Furth and Rosenbluth,[5] Eq. (3) grossly over-estimates radial orbit widths in the presence of significant charge density. Thus radial gradients in the $E \times B$ drift, arising from radial gradients in E_r and therefore proportional to the local charge density, have long been known to modify guiding-center motion. For realistic sheath values of dE_r/dr the result is "orbital squeeze": a pronounced shrinkage in radial width of the ion orbit. (The effect on electron orbits is negligible.) It can be shown that similar squeezing will also typically occur in the idealized case of a uniform magnetic field, where it is manifested by elliptical Larmor orbits.

In other words, a magnetically confined plasma is typically characterized by a "skin," on its radial periphery, of squeezed orbits. The importance of this skin with regard to plasma-wall interaction was first mentioned in Ref. 5.

A second reason for the unrealistically large predictions of naive orbit theory is less obvious, but equally important. It is rooted in the fact that the sheath or halo region, containing a significant plasma density (a per cent or so of the central density), is not collisionless. While it may approach (as in the TEXT device) or enter the "banana" regime of neoclassical theory, collisional processes remain important well beyond the banana-plateau

transition. In the context of halo physics, collisions are primarily important because they imply relaxation of poloidal rotation.[6,7] For the relatively large sheath electric fields, $E \times B$ poloidal rotation is potentially large, and its decay through collisional viscosity has striking effects. We shall show that collisional relaxation, in concert with the orbital squeeze, further reduces sheath electric fields.

A secondary consequence of collisions is to reduce the population of banana particles. In the TEXT device, for example, one finds that a sizable fraction of the halo ions are insufficiently energetic to execute their collisionless orbits. Since collision-dominated ions do not contribute to space charge, the sheath field is again reduced.

It should be clear that understanding the structure of the radial sheath is not possible without *self-consistent* analysis of guiding-center motion, collisional relaxation and Poisson's equation. In the case of orbits, for example, we note that variation of the radial sheath potential can squeeze ion radial excursions, thereby attenuating the halo space-charge. Too much orbital squeeze, corresponding to ion orbits little wider than their electron counterparts, would inconsistently eliminate the source of the charge density; too little dE_r/dr would yield little shrinkage and an inconsistently potent halo.

It should also be clear that the radial sheath, which achieves equilibrium only through orbit modification, has a peculiar and novel structure. Especially when guiding center orbits have macroscopic dimension (such as

tokamak banana orbits), it is described by a self-consistency condition entirely unlike the axial case. The radial sheath equation is nonlocal (integro-differential). Even its lowest-order, localized version is distinct: we shall find that approximation to be a transcendental equation for $d^2\phi/dr^2$ alone, rather than a differential equation for ϕ as in the axial case.

The present derivation and analysis of the radial sheath equation, based on a simplified kinetic theory, is highly idealized. Its intention is to display the key features of radial sheath structure—ion halo, orbital squeeze, rotation and self-consistency—in the simplest possible context. Yet when the (non-adjustable) parameters of the model are fitted to values characterizing the TEXT edge region, we find the main features of the experimental electrostatic field to be reproduced, within factors of two or three. In other words, self-consistency alone is sufficient for a prediction in reasonable agreement with experiment.

It is convenient to point out here that the present, essentially kinetic description of halo physics is by no means the only plausible description. Indeed, a sheath theory based on scalar-pressure fluid equations has long been available.[8] This alternative analysis takes into account the conducting nature of the limiter surface and, unlike the present work, treats seriously the variation of electron temperature within the sheath.

We also point out that the present analysis specifically addresses a poloidal limiter. The sheath analysis corresponding to a toroidal limiter would dif-

fer because of the different ways in which orbits are interrupted in the two limiter geometries.

In the following section we briefly consider the ion halo and review the influence of space charge on tokamak guiding-center orbits. The orbital squeeze is discussed from a general point of view as well as in the local approximation of previous theory. Collisional processes—especially the decay of poloidal rotation—are reviewed in Sec. III. In Sec. IV we derive the self-consistent radial sheath equation. Model distribution functions are used to make the equation explicit and extract its local approximation. The numerical solution to this transcendental equation is displayed and compared to TEXT data in Sec. V. Our conclusions are summarized in Sec. VI.

II. Space Charge and Guiding-center Orbits

The density of a magnetized plasma species, when viewed on time scales long compared to its Larmor period, cannot vary arbitrarily over spatial scales shorter than its thermal gyroradius. Because (for comparable species temperatures) $\rho_i \gg \rho_e$, the ion density in a magnetized plasma is relatively fuzzy; it cannot track abrupt changes—specifically, sharp changes in slope—in n_e. (It is not hard to see that an ion density of constant slope is easily constructed, independent of the magnitude of the slope.) Thus whenever the plasma boundary tends to induce large d^2n_e/dr^2, a charge halo should be expected.

A similar but more severe halo is pertinent to a toroidally confined plasma. Here the relevant orbit corresponds to guiding-center motion, rather than Larmor gyration, and the time scale of observation must be presumed long compared to the bounce or transit period. On such time scales, any charged particle is effectively smeared over the generally macroscopic extent of its guiding-center orbit. Note that in this case rapid equilibration along the magnetic field allows only a radial halo—one bounded by flux surfaces.

The simplest example is banana motion in a tokamak; the conventional banana has radial width

$$\left(\frac{r}{R}\right)^{1/2} \rho_p \approx \rho_p \gg \rho,$$

in view of Eq. (2). We note here that

$$\frac{B}{B_p} = \frac{Rq}{r}, \tag{4}$$

where q is the safety factor. This factor is close to 12 in typical tokamak geometry, intensifying the (non-self-consistent) halo over what would be expected in the slab case. Denoting the self-consistent, squeezed orbit-width by Δ, and recalling the qualitative argument of Sec. I, we presume

$$\Delta_i \gg \Delta_e.$$

A straightforward way to guarantee quasineutrality in the plasma interior is to assume that ion and electron banana centers have identical spatial distributions, both vanishing at the limiter radius (because electrons with orbital

centers outside $r - a$ do not survive). Then the electron charge density vanishes within Δ_e of $r = a$, while n_i decays over the much broader range of Δ_i, yielding the expected halo of positive charge. Below we refer to this simple alignment of ion and electron orbital centers as "guiding-center neutrality" (although "guiding-center *quasi*neutrality" would be more accurate).

Clearly other distributions are possible; a precise alignment of electron and ion orbital-centers in the region immediately interior to $r = a$ is not compelling. But it should be stressed that the halo not easily filled by electrons. Because of ambipolarity, the relative disposition of ion and electron banana-centers in the vicinity of the limiter radius is severely constrained. Recall that orbital centers move radially in response to dissipative processes, which typically conserve local momentum (this applies to both Coulomb collisions and the most probably relevant turbulent diffusion processes). As a result, the radial motion of electrons and ions are tightly linked; only electron-ion pairs can enter the halo region. Of course such pairs have no effect on the halo charge density.

Other potential sources of halo charge, such as ionization, are also inherently ambipolar, and thus irrelevant. A prominent exception is secondary emission of electrons from the limiter plate, a process that can clearly contaminate the halo with additional electrons. Without attempting an *a priori* accounting of secondaries, we note experimental evidence that they do not dominate halo physics. Measured sheath potentials are roughly symmetrical

with respect to the limiter radius—an improbable symmetry if secondary emission, restricted to the $r > a$ region, were controlling the space charge.[2] Thus, while secondary electrons and other departures from guiding-center neutrality would enter a complete radial sheath analysis, the main sheath features should be visible in the guiding-center-neutral case.

Next consider the guiding-center orbits. We have already noted that rapid electron streaming annihilates asymmetry outside a thin Debye sheath at the limiter, so the halo region is effectively axisymmetric. For the same reason poloidal variation of the sheath potential, mainly a response to finite aspect-ratio and plasma rotation, is relatively small. The essential features of sheath structure involve only the dominant part of ϕ, which is a function of minor radius only.

Using these simplifications and large aspect-ratio

$$\frac{r}{R} \ll 1,$$

we can exploit previous studies tokamak orbits.[4,5] We briefly review, with mild generalization, the previous work. The invariant angular momentum can be expressed as

$$p_\zeta = mRv_{||} - \frac{e\chi}{c}, \tag{5}$$

where ζ denotes the toroidal angle, m is the particle mass, $v_{||}$ the parallel speed and χ is the poloidal flux. We have used Eq. (3) to ignore the distinction between the field magnitude B and its toroidal component, B_T,

whence

$$v_{\|\zeta} \approx v_{\|}.$$

The contribution of perpendicular drifts to the toroidal speed is omitted because of the small gyroradius ordering

$$\rho \ll L,$$

where L can be identified with the radial scale-length of sheath variation. It is significant that ρ and not ρ_p appears here; we explicitly allow for variation of sheath parameters on the scale of ρ_p. (The variation observed in the TEXT sheath approaches this steep scale.)

Poloidal guiding-center motion results from streaming as well as poloidal $E \times B$ drifts,

$$v_p = \frac{B_p}{B} v_{\|} + V_{Ep} = \frac{B_p}{B} v_{\|} - \frac{cE_r}{B}.$$

The $\mathbf{V}_E \equiv (c/B)\mathbf{E} \times \mathbf{B}$ term is retained here, despite its neglect in (5), because B_p/B is small in the inverse aspect ratio. It is also worth recalling that $E \times B$ motion is an exact consequence of the Lorentz force, and not exclusively a small ρ/L effect.

Trapped particles, which have a special influence on the sheath potential, satisfy $v_p(r_b, \theta_b) = 0$ at some bounce radius r_b and bounce angle θ_b. Introducing the abbreviation

$$U(r) = \frac{cE_r(r)}{B_p}, \tag{6}$$

we can write

$$v_{||}(r_b, \theta_b) = U(r_b). \tag{7}$$

It is convenient to denote the orbital change of any quantity $r(r, \theta)$ by

$$\Delta f = f(r, \theta) - f(r_b, \theta_b).$$

Then $\Delta p_\zeta = 0$ implies

$$mR\Delta v_{||} + mv_{||}\Delta R - \frac{e}{c}\chi'\Delta r = 0.$$

Since $B_p = \chi'/R$ and $\rho_p = v\text{th}/(eB_p/mc) = v_{\text{th}}/\Omega_p$, where v_{th} is the thermal speed, we can express momentum conservation as

$$\Delta v_{||} = \Omega_p \Delta r - \frac{U(r_b)\Delta R}{R}, \tag{8}$$

where

$$\Delta v_{||} = v_{||} - U(r_b). \tag{9}$$

Note that Δr is the orbital width and recall that

$$\frac{\Delta R}{R} = O\left(\frac{r}{R}\right)$$

is presumed small. Similar manipulation of the energy conservation law,

$$\Delta\frac{mv_{||}^2}{2} = \frac{\mu B}{R}\Delta R - e\Delta\phi,$$

where μ is the invariant magnetic moment and we have used

$$\Delta B \approx -B\frac{\Delta R}{R},$$

yields the relation

$$\Delta v_{\|}\left(U_b+\frac{\Delta v_{\|}}{2}\right)=\frac{\mu B}{m}\frac{\Delta R}{R}-\frac{e\Delta\phi}{m}, \tag{10}$$

where $U_b \equiv U(r_b)$. When ϕ varies moderately on the scale of the radial orbit width, it is appropriate to expand

$$\begin{aligned}-\frac{e\Delta\phi}{m} &= -\frac{e}{m}\left[\phi_b+\phi_b'\Delta r+\frac{\phi''\Delta r^2}{2}+\cdots\right] \\ &= \Omega_p\left[U_b\Delta r+\frac{U_b'\Delta r^2}{2}+\cdots\right]\end{aligned} \tag{11}$$

as in the previous literature. However, allowing for faster ϕ-variation, we defer this step and neglect only Δr^2 to write, combining (8) and (10),

$$\Delta r\left[\Delta r+\frac{2U_b}{\Omega_p}\left(1-\frac{\Delta R}{R}\right)\right]+\rho_p^2\Delta\frac{e\phi}{T}=\frac{2\mu B}{m\Omega_p^2}\frac{\Delta R}{R}. \tag{12}$$

The left-hand side of this relation is a function of Δr that vanishes at $\Delta r = 0$, while the right-hand side is effectively independent of Δr and of order $\rho_p^2(r/R)$. There are three possibilities:

(i) When ϕ varies slowly, as in the plasma interior, the first term on the left-hand side dominates and the orbit has the conventional width $\Delta r \sim (r/R)^{1/2}\rho_p$.

(ii) ϕ may vary so rapidly that the second term on the left-hand side dominates; notice that in this case we have

$$\Delta\frac{e\phi}{T}=O\left(\frac{r}{R}\right) \tag{13}$$

the general expression of the orbital squeeze. The only way Eq. (13) can be satisfied in the presence of sharp potential gradients is by radial shrinkage of each banana orbit.

(iii) In the intermediate case, the two terms on the left may be comparable. In particular, the sense of $\Delta\phi$ may allow the two terms to nearly cancel at certain radial regions. This singular possibility has been considered in some detail elsewhere[12]; it yields orbits that encircle the magnetic axis as in the untrapped case, without straying far from a single flux surface.

While the singular cancellation is approached at the extremities of the radial sheath, we do not consider it further here. Its effects are too radially localized to critically influence sheath structure, at least in the limiter case of present concern. Our attention below is concentrated on case (ii), which will be seen to describe most of the sheath region.

Next we turn to the local approximation of Eq. (11). A striking new feature is the cancellation of the lowest order term, $\Omega_p U_b \Delta r$, from Eq. (12). Furthermore, since the two terms in (8) are comparable, $\Delta v_{||} = O(r/R)$ and it is consistent to replace U_b by $v_{||}$ wherever it is multiplied by r/R. Hence we obtain the localized orbit equation

$$\left[\Delta r - \frac{v_{||}}{\Omega_p}\frac{\Delta R}{R}\right]^2 - \frac{U_b'}{\Omega_p}(\Delta r)^2 = \frac{2}{\Omega_p^2}\frac{\Delta R}{R}\frac{(\mu B + v_{||}^2)}{m}, \qquad (14)$$

which is easily solved for Δr. The fact that only U_b' and not U_b (i.e., ϕ'' and not ϕ') appears here is related to Galilean invariance.[10]

For our purposes the following abbreviated version of Eq. (14) is sufficient. Let Δr_0 denote the conventional banana width:

$$\Delta r_0 \equiv \Delta r(U_b' = 0).$$

Then the squeezed orbit is evidently described by

$$\Delta r^2 = \frac{\Delta r_0^2}{S},$$

where the squeeze factor is

$$S \equiv \left|1 - \frac{U_b'}{\Omega_p}\right|. \tag{15}$$

The first observation concerning S is that its departure from unity is proportional to particle mass. Hence, for any reasonable squeezing of ion orbits, we have

$$S_e = 1 + O\left(\frac{m_e}{m_i}\right):$$

squeezing of electron orbits does not occur. We exclusively consider ion orbits from here on, often suppressing the i-subscript. Other critical features of S are visible from the expression

$$S = \left|1 + \frac{c\phi''}{B_p\Omega_p}\right| = \left|1 + \frac{1}{2}\rho_p^2\frac{e\phi''}{T_i}\right|. \tag{16}$$

We point out that:

(i) A crude estimate from TEXT data suggests

$$S \sim 10. \tag{17}$$

The point here is that ϕ and ϕ' have different scale lengths. If we define

$$r_\phi \equiv \left[\frac{d \ln \phi}{dr}\right]^{-1},$$

where the slope is measured near its maximum, a centimeter or two from the peak, then the observations suggest that

$$\phi'' \gg \frac{\phi}{r_\phi^2},$$

at the peak.

We will find that the estimate (17) also follows from self-consistency. It is therefore worth mentioning that its inference from the TEXT data is only marginally justified by the experimental resolution. It is not used as a critical test of the present analysis.

(ii) The ϕ'' term is negative in the positive halo of the radial sheath. This circumstance alters banana geometry and implies that edges of the sheath will enter the singular region, as discussed previously. While the singularity at $S = 0$ is not physical—the local approximation breaks down before S becomes small—we must keep in mind that a local analysis remains accurate only while S exceeds unity.

(iii) Our general conclusion concerning the orbital squeeze, Eq. (13), is easily made explicit in the local case. From the local approximation we have found that $\Delta r^2 \leq \epsilon \rho_p^2 / S$. At the sheath center we have $\phi' \approx 0$ and $\Delta\phi \approx \phi'' \Delta r^2/2$, whence

$$\Delta\left(\frac{e\phi}{T}\right) \approx \frac{S\Delta r^2}{\rho_p^2} \leq \epsilon,$$

as before: the orbit squeezes to maintain the bound on $\Delta\phi$.

III. Collisional Relaxation

It is easily appreciated that the shrinkage of collisionless ion orbits has the effect of reducing halo space charge. However, Coulomb collisions have equally important effects on radial sheath structure, for two reasons. First, sufficiently frequent collisions prevent the execution of banana orbits, removing the essential cause of charge imbalance. Such orbit randomization occurs whenever the effective collision frequency, ν_{eff}, equals or exceeds the trapped particle bounce frequency, ω_b; it is marginally relevant in TEXT, where ν_{eff} and ω_b are comparable in the halo region.

The second consequence of collisions, rotational relaxation, is more generally important, affecting space charge even when $\nu_{\text{eff}} \ll \omega_b$. For this reason we consider rotational relaxation in some detail here; orbit randomization is treated in the experimental comparison presented in Sec. V.

To begin we review some well-known features of the interior region in

a banana-regime tokamak.[11] Because $\nu_{\text{eff}} \ll \omega_b$, guiding-center orbits are collisionless, displaying the well-known banana excursions. However, the *distribution* of such orbits is far from collisionless. Because the particle confinement time is much longer than ν_{eff}—fundamentally, because of scale-length orderings—the guiding-center distribution function is a Maxwellian in kinetic energy, whose radial profile is determined by collisional dissipation.

The relevant scale-length ordering here is

$$\frac{\Delta}{L} \ll 1,$$

where Δ is as usual a radial orbit width and L a scale-length for macroscopic variation. Whenever the neoclassical ordering,

$$\frac{\Delta}{L}\omega_b \ll \nu_{\text{eff}}, \tag{18}$$

is satisfied, then Δ/L is the primary small parameter. Independently of the collisionality $\nu_{\text{eff}}/\omega_b$, Eq. (18) forces the lowest order distribution function, f_0, to be a local Maxwellian; collisionless motion determines only the first-order correction, $f_1 = O(\Delta/L)$.

The ordering (18) has striking consequences in the presence of strong radial electric fields.[6] In that case, collisional viscosity acting on the poloidal $E \times B$ drift has been shown to quickly relax the poloidal flow,

$$V_p \;=\; O\left(\frac{\rho}{L}\right),$$

by inducing a mean flow along $\mathbf{B}$:

$$V_p \;=\; V_{\|p} + V_{Ep} \approx \frac{B_p}{B} V_{\|} - \frac{cE_r}{B} \approx 0.$$

The corresponding toroidal flow is relatively fast:

$$V_t \;\approx\; V_{\|t} = \frac{cE_r}{B_P} \gg V_E$$

After comparison with Eq. (6), we can express the basic fact of tokamak rotation very simply: at each radius, there occurs collisional relaxation to a local Maxwellian centered in parallel velocity at U:

$$f_0(r, \mathbf{v}) \propto \exp\left[-\frac{v_\perp^2 + v_\|'^2}{v_{\rm th}^2}\right], \tag{19}$$

where

$$v_\|' \equiv v_\| - U(r). \tag{20}$$

We note that Eq. (19) is an elementary prediction of neoclassical theory, requiring little more than that the underlying collisional process satisfy an H-theorem.

So far this discussion has reviewed well-known features of rotating-plasma equilibrium in the tokamak interior. But it is not hard to see that essentially the same conditions and arguments pertain in the radial sheath. In particular, the basic ordering (18) appears to describe most tokamak sheaths, including H-mode discharges where the edge is relatively hot, mainly because orbital squeezing keeps the scale-length ratio small. It is easily satisfied in the TEXT radial sheath.

In fact, at least in the case of TEXT, the main distinguishing feature of the edge region is that the electric field is directly measurable and large. From TEXT[2] data one finds

$$U \sim \frac{1}{2} v_{\mathrm{thi}}.$$

Hence the inclusion of the toroidal flow term, as in Eq. (19), adds significant realism to any analysis of the limiter region. It should be emphasized, however, that local collisional relaxation can occur only over radial scales long compared to the orbit width. Thus Eq. (19) consistently describes the sheath region only because banana orbits are squeezed.

IV. Radial Sheath Equation

Let $r_0(\mathbf{v})$ denote some average radius of the guiding-center orbit of a halo ion having velocity $\mathbf{v}$, and let $g(r_0, \mathbf{v})$ denote the distribution of such orbits. Thus, in particular, g prescribes which banana orbits are populated and which are not. We can then express the distribution of halo ions as

$$f(r, \mathbf{v}) = g\left[r - (r - r_0), \mathbf{v}\right]. \tag{21}$$

We call f the halo distribution to allow for other, charge-neutral ion populations in the sheath region. As emphasized in Sec. I, the region outside the limiter contains a background of neutral plasma (presumably reflecting transit-time residence and ionization): the space-charge decays to zero before the plasma density.

We calculate the halo-ion density, $n(r)$, by adopting a simple model for g, and then evaluating the integral

$$n(r) = \int d^3v\, g[r - (r - r_0), \mathrm{v}]. \tag{22}$$

The simplest model for g has a linear dependence on r_0. We suppose that that no ion whose orbital center is outside the limiter radius survives,

$$g(r_0) = 0, \quad r_0 \geq a, \tag{23}$$

and that the distribution of orbital centers inside the limiter decreases linearly:

$$g(r_0) = \left[\frac{a - r_0}{r_n}\right] f_0, \quad r_0 < a. \tag{24}$$

Hence f_0 is the function of v specified by Eq. (19) and r_n is a density-gradient scale length pertinent to the sheath region.

This linear model for g is obviously not unique. Other models have been considered, including one, with a Gaussian profile in radius, that yields a somewhat more realistic sheath potential. However, we have not found the model choice to have a crucial bearing on final results, and Eqs. (23) and (24) have advantages with regard to simplicity and clarity: they seem in some sense the archetypal choice. Moreover, the experimental density measurements are sufficiently consistent with Eq. (24) that r_n can be estimated from the data.[12]

Similarly the choice of r_0 is not unique; as long as the scale r_n is wide compared to the orbit width, different choices of r_0 will yield indistinguishable

halo densities. For convenience of integration, Eq. (19) suggests choosing r_0 as that radius in which the parallel velocity in the moving frame vanishes:

$$v'_{||}(r_0) = 0.$$

It is then a simple matter to deduce from Eq. (5) the formula

$$r - r_0 = \frac{v'_{||}}{\Omega_p} + \frac{[U(r) - U(r_0)]}{\Omega_p}, \tag{25}$$

or in the local approximation,

$$r - r_0 = \frac{\pm v'_{||}}{\Omega_p S}, \tag{26}$$

where S is the squeeze factor of Eq. (15). Here the sign is irrelevant because f_0 is even in $v'_{||}$.

The distribution implicit in Eqs. (21), (24) and (26) can also be derived from a simplified but formally conventional neoclassical argument. While the neoclassical argument makes our result no more compelling, it casts some light on our omissions. The

drift-kinetic equation,

$$(\mathbf{v}_{||} + \mathbf{v}_D) \cdot \nabla f = C(f, f) \tag{27}$$

is to be solved for small Δ/L as discussed in Sec. III. The lowest-order solution is a local Maxwellian in the rotating frame. The banana-regime correction, f_1, is chosen to approximately preserve the invariant p_ζ or, equivalently, r_0:

$$f(r, \mathbf{v}) = f(r_0) = f(r) - (r - r_0) f'(r).$$

Indeed one finds that $f_1 = -(r-r_0)f_0'(r)+G(r)$, where f_0 is given by Eq. (19). The function G is ultimately determined by collisions. Here we recall only its crucial property: G tends to cancel the first term of f_1, $-(r-r_0)f'(r)$, except in the trapped particle region.[11] As a result most neoclassical effects are proportional to $(2r/R)^{1/2}$, the relative volume of trapped phase space.

Thus the drift-kinetic equation gives results roughly consistent with the model of Eq. (21) *et seq.* On the other hand, some of the simplifications of that model are now especially clear. In addition to omitting temperature and other gradients implicit in f_0', we have neglected the phase-space localization implicit in the function G. On the other hand the missing phase-space factor $(2r/R)^{1/2}$ is close to unity for realistic aspect ratios.

Returning to the linear model, we combine Eqs. (23), (24) and (26) to evaluate the integral in Eq. (22). The result is

$$n(r) = \frac{n_0}{2r_n}\left\{a - r + |a-r|\mathrm{erf}(Sx) + \frac{\rho_p}{S\sqrt{\pi}}\exp(-S^2x^2)\right\}, \qquad (28)$$

where n_0 is a constant measure of the halo density and

$$x = \frac{|a-r|}{\rho_p}. \qquad (29)$$

This density decays properly for $r - a \gg \Delta \sim \rho_p/S$; for $r - a \ll \Delta$, in the plasma interior, we find $n \to (n_0/r_n)(a-r)$, a large charge which must be cancelled by n_e. Hence we choose

$$n_e = \frac{n_0}{r_n}(a-r)\Theta(a-r)$$

consistently with both guiding center neutrality, as discussed in Sec. II, and the vanishingly small electron gyroradius (a finite gyroradius version is easily constructed and found, unsurprisingly, to give indistinguishable results). Here of course Θ is a step-function. We have derived the halo charge density

$$n_i - n_e = \frac{n_0 \rho_p}{2 S r_n} \left[\frac{1}{\sqrt{\pi}} \exp\left(-S^2 x^2\right) - Sx \operatorname{erfc}(Sx) \right]. \tag{30}$$

Before combining it with Poisson's equation,

$$\phi'' = -4\pi e (n_i - n_e),$$

we note that Eq. (16) implies

$$S = -1 - \frac{1}{2} \rho_p^2 \frac{e\phi''}{T_i},$$

whenever the right-hand side is positive—the important case, in view of (17). Hence we have

$$S + 1 = \frac{\rho_p^2}{2\lambda_D^2} \frac{T_e}{T_i} \frac{n_i - n_e}{n_0},$$

where the Debye-length is defined in terms of n_0:

$$\lambda_D^2 = \frac{T_e}{4\pi n_0 e^2}.$$

The radial sheath equation can therefore be expressed as

$$\delta S(S+1) = F(Sx), \tag{31}$$

where δ is the radial sheath parameter

$$\delta \equiv \frac{4 r_n}{\rho_p} \left(\frac{\lambda_D}{\rho_p} \right)^2 \frac{T_i}{T_e}, \tag{32}$$

and, from Eq. (30),

$$F(y) \equiv \frac{1}{\sqrt{\pi}} \exp\left(-y^2\right) - y\,\mathrm{erfc}(y).$$

Equation (31) is to be solved for S as a function of radius x. Before considering the numerical solution $S(x)$, we comment on salient features of the equation.

The radial sheath equation is a transcendental equation for S, rather than a differential equation for F, as in the axial case. The reason for this difference has been discussed previously: in the axial case, ϕ'' depends on ϕ because particle streaming normal to the boundary equilibrates to the local potential; in the radial sheath, where the relevant particle motion involves guiding center drifts and where radial profiles are determined by slow-time-scale collisional relaxation, only changes in ϕ' are relevant.

The local approximation pertains only near the center of the sheath, as noted in Sec. II. A more broadly accurate sheath equation, based on Eq. (25) rather than Eq. (26), would have the form

$$U' = N[\Delta U; x], \tag{33}$$

where N is a non-local functional of $\Delta U = U(r) - U(r_0)$. Equation (31) should be viewed as the first approximation, valid near the potential peak where U is indeed linear, to this more general version. The local approximation explains in particular why Eq. (31) fails to satisfy $S \to 1$ for $|x| \to \infty$;

indeed, $S+1$ is proportional to the charge density only when the latter is sufficiently large. It is therefore consistent to replace $S+1$ by S on the left-hand side of (31); equivalently, we have

$$S \cong -\frac{1}{2}\rho_p^2 \frac{e\phi''}{T_i}. \tag{34}$$

The sheath parameter has the alternative expression

$$\delta = \frac{r}{R}\frac{r_n}{\rho_p}\left(\frac{v_A}{qc}\right)^2, \tag{35}$$

where v_A is the local Alfvén speed and q the safety factor. For TEXT sheath conditions we find

$$\delta \sim 10^{-2} - 10^{-3}.$$

It is smaller in H-mode discharges, where the edge temperature is relatively large and r_n relatively small.

Certain idealizations of our model are visible here and worth emphasis. For example, Eq. (31) is symmetrical in $(r-a)$, implying that ϕ decays identically in the limiter shadow and the plasma interior. As noted in Sec. II, the experimental data roughly preserves this symmetry. Equation (35) is explicitly model dependent in the appearance of the density gradient scale-length; recall from Sec. II that only d^2n/dr^2 should enter the halo charge density. The point is that our model has constant density outside the limiter radius, so that r_n in fact measures a second derivative. The Gaussian model has continuous slope; it yields a similar sheath parameter where r_n is replaced

by

$$r_n \to \left[\frac{n}{(d^2n/dr^2)}\right]^{1/2}.$$

V. Solution and Experimental Comparison

The non-self-consistent charge density is found by setting $S = 1$ in Eq. (30). The corresponding fields and potential can be found by integration; as noted previously they overstate the observed field by about two orders of magnitude.

Turning to the self-consistent case, we observe (from the monoticity of both members) that Eq. (31) has a unique solution for each radial position, x. We denote this solution, which assumes every ion to complete its collisionless orbit, by $S_*(x)$; it is easily found numerically.

Note in particular that

$$S_*(0) \cong \pi^{-1/4}\delta^{-1/2}$$

is indeed large; for typical experimental data one finds

$$S_*(0) \cong 15\text{–}20.$$

Hence Eq. (34) is pertinent and we can determine the electrostatic field from straightforward integration. For example

$$\frac{eE_r}{T_i} = \frac{2}{\rho_p}\int dx\, S(x), \tag{36}$$

where $x = |r - a|/\rho_p$ and the integration constant is fixed by $E_r(0) = 0$.

Since the local approximation breaks down a few gyroradii from $r = a$, the asymptotic, $x \to \infty$, limit of S is not physical. Yet S does become relatively small for $x \sim 3$; Figure 1 shows that the electric field in this region is nearly constant. In other words it is possible to discern an asymptotic E_r, which changes relatively slowly; we denote this quantity, which provides a useful datum for experimental comparison, by E_0:

$E_r \to E_0 \approx$ constant, at sheath edge.

One finds that the E_0 computed from S_* is much closer to the observations than the non-self-consistent version; however it remains larger, by roughly a factor of 6, than the experimental asymptotic field.

The reason for this disparity was discussed in Sec. III, where it was noted that ν_{eff} and ω_b are comparable in the limiter scrape-off of TEXT. Because only the hotter ions are able freely to execute banana orbits in this case, our halo integral overestimates the ion charge density. We adopt a crude but transparent remedy, simply excluding from the halo integral any ion whose energy is too low to satisfy the banana constraint $\nu_{\text{eff}}(v)/\omega_b(v) < 1$, where the two factors on the right are the *velocity-dependent* effective collision frequency and bounce frequency respectively. Note that this criterion is a strong function of v, since $\nu_{\text{eff}}(v)/\omega_b(v) \propto v^{-4}$. Explicitly, we define the critical speed v_c by

$$\nu_{\text{eff}}(v_c)/\omega_b(v_c) = 1,$$

and cut off the halo integral for speeds lower than vc:

$$\int_0^\infty dv \to \int_{v_c}^\infty dv.$$

While this treatment of collisional randomization is far from rigorous, it is difficult to believe that more elaborate analysis would yield significantly different results. Since the slower particles make smaller excursions, the cut-off affects S only very close to the limiter radius. Even at $r = a$ the effect is only moderate; the corrected $S(0)$ is ten or twelve, so that, in particular, Eq. (34) remains valid. Nonetheless the total halo charge is diminished enough to significantly improve the prediction for E_0.

Figure 1 shows the resulting electrostatic sheath potential $\phi(x)$, compared to five experimental measurements from a single TEXT run. The agreement between theory and experiment is on the whole quite good. Note the asymmetry of the experimental points, which show a depressed charge density in the limiter shadow; such asymmetry is also evident—if less striking—in other experimental runs. It is quantitatively moderate (less than 15%) and hardly surprising in view of the likely presence, for $r > a$, of unneutralized secondary electrons, as discussed in Sec. II. In the region $r < a$, where our idealizations would be expected to be more realistic, theory and experiment are especially close.

In addition to experimental uncertainty (discussed in Ref. 2), Fig. 1 is subject to imprecision concerning the value of the sheath parameter, δ.

In particular, in order to estimate the value of $n/r_n = dn/dr$ for the halo ions just inside the sheath, one must first estimate the relative proportions of halo ions and charge-neutral background ions. We use the relatively constant density in the limiter shadow as an estimate for the latter,[11] and conclude that the two ion populations are roughly comparable. Fortunately it can be shown that the gross features of sheath structure, including E_0, are very weak functions of δ.

A more precise comparison of theory and experiment is based on E_0. The data allow reasonably unambiguous measurement of this field, which is also straightforwardly computed from Eq. (36)—using, of course, the collisionally corrected S. The resulting comparison is robust in the following ways: (i) it depends only weakly on δ; (ii) it is remarkably similar over several sets ("runs") of TEXT data; (iii) it is roughly the same for the Gaussian and linear halo-density models. One finds that the theoretically predicted E_0 exceeds the experimental asymptotic field by a factor of two or three—more commonly three:

$$E_0(\text{theory}) \approx 3 \cdot E_0(\text{experiment}). \tag{37}$$

We ascribe this disagreement to electron contamination of the sheath, or, equivalently, to inadequacies of our model for the halo charge. In fact such assumptions as guiding-center neutrality and Eq. (27) seem sufficiently idealized to make the agreement expressed by Eq. (37) its most striking feature. In this regard it should be emphasized that the non-self-consistent

prediction, for the same δ, is about 80 times larger:

$$E_0(\text{non-self-consistent}) \approx 250 \cdot E_0(\text{experiment}). \tag{38}$$

Equations (37) and (38) express concretely the critical importance of such self-consistent processes as orbital squeezing and rotational relaxation to the structure of the radial sheath.

We close this section with some remarks on the calculation of E_0. Denoting its dimensionless measure by

$$\widehat{E} = \int_0^{x_0} dx\, S(x),$$

we introduce the integration variable $y = S(x)x$. Then the sheath equation becomes

$$S(S+1) = \frac{F(y)}{\delta}, \tag{39}$$

and furthermore, we have

$$\frac{dx}{dy} = \frac{1}{S} - \frac{(y/S^2)dS}{dy}.$$

Then

$$S\frac{dx}{dy} = 1 - \frac{yd(\ln S)}{dy},$$

so the integral for $\widehat{E}$ can be written as

$$\widehat{E} = \int_0^{y_0} dy \left[1 - yd\frac{\ln S}{dy}\right] \tag{40}$$

where $y_0 = y(x_0)$. Since S can be expressed in terms of y using Eq. (39), Eq. (40) gives an explicit expression for $\widehat{E}$, which can be evaluated without solving the sheath equation.

Our sole application of Eq. (40) is to study the dependence of $\widehat{E}$ on the sheath parameter δ. It is noteworthy that δ enters (40) only through the integration endpoint, which is chosen such that $S(x_0) \approx 1$. Using this fact and assuming $\delta \ll 1$, one finds from (40) that

$$\widehat{E} \propto (\ln \delta)^{3/2};$$

as remarked previously, such weak dependence is roughly consistent with the experimental data. A more important dependence of sheath structure on edge parameters comes from Eq. (39), which provides scaling for the maximum orbital squeeze:

$$S(0) \sim \delta^{-1/2} \sim B_p^{3/2}.$$

VI. Summary

We have studied the radial sheath observed near the limiter radius in the TEXT tokamak. We have shown that self-consistency, manifested through both the radial squeezing of ion guiding-center orbits as well as the radial variation of $E \times B$-induced toroidal rotation, is the critical issue for sheath structure. Indeed, reasonable agreement with experiment is obtained from an idealized model which, however simplified, preserves such self-consistent

effects. This conclusion is visible in Fig. 1 and quantitatively expressed in Eqs. (37) and (38).

The salient features of the sheath considered here are generally pertinent. A radial sheath occurs whenever the plasma boundary is a flux surface—whenever, as in most confinement devices, the confining field lines lie in the bounding surface. The present work suggests that most such sheaths, including those associated with separatrix (divertor) geometry, should be broadly similar. Only the collision-dominated sheath, in which the disparity in radial width between electron and ion orbits cannot induce charge separation, seems significantly distinct. In larger, hotter tokamak plasmas, where the edge region is more fully collisionless and has steeper density gradients, the effects studied here would be magnified.

The radial squeezing of ion banana orbits is of special importance. We have emphasized its importance to theoretical consistency: the relaxation of plasma rotation occurs only on scales wider than an ion banana, and could not affect sheath structure if the bananas were not squeezed. The orbital squeeze seems even more relevant to tokamak burning-plasma experiments, since fusion products must penetrate a skin of thin bananas before striking the container wall or reaching a divertor. Since alpha-particle orbits are also squeezed (in fact somewhat more than proton orbits), an estimate of wall bombardment that omitted radial-sheath physics would be seriously in error.

Finally we have argued that the radial sheath is an object of some intrinsic interest. It is fundamentally distinct from the more familiar axial sheath, essentially because magnetized charges respond very differently to parallel and perpendicular electric fields. As a result its structure is determined, in lowest approximation, by a transcendental self-consistency relation for the charge density, rather than a differential equation for the potential. Moreover, the predictions of this equation are realistic only when it incorporates both self-consistent orbit modification and the collisional processes pertinent to a $E \times B$ driven rotation. At least in the parameter regimes typical of modern tokamak experiments, equilibration of the radial sheath depends upon a peculiar interplay between collisionless and collisional physics.

Acknowledgements

The author is indebted to scientists in the TEXT experimental group, especially Ch. P. Ritz, R. Bengtson, P. Schoch and A. Wootton, not only for generously sharing TEXT data, but also for crucial early advice. The author also wishes to thank D.E. Baldwin, H.L. Berk, P.J. Morrison and F.L. Waelbroeck for helpful criticism and encouragement. This work was supported by the U.S. Department of Energy, Grant # DE FG05-80ET 53088.

References

1. See, for example, D. Bohm in *The Characteristics of Electrical Discharges in Magnetic Fields*, edited by A. Guthrie and R. K. Wakerling (McGraw-Hill Book Company, Inc., New York, 1949), Chapter III.

2. Ch. P. Ritz, D. L. Brower, T. L. Rhodes, R. D. Bengtson, S. J. Levinson, N. C. Luhmann, Jr., W. A. Peebles, and E. J. Powers, Nuc. Fusion **27**, 1125 (1987).

3. Ch. P. Ritz, R. D. Bengtson, S. J. Levinson, and E. J. Powers, Phys. Fluids **27**, 2956 (1984).

4. H. L. Berk and A. A. Galeev, Phys. Fluids **10**, 441 (1967).

5. H. P. Furth and M. N. Rosenbluth, in *Plasma Physics and Controlled Nuclear Fusion Research*, (IAEA, Vienna, 1969), Vol. 1, p. 821.

6. F. L. Hinton and S. K. Wong, Phys. Fluids **28**, 3062 (1985).

7. A. B. Hassam and R. M. Kulsrud, Phys. Fluids **21**, 2271 (1978).

8. See, for example, V. G. Petrov, Nucl. Fusion **24**, 259 (1984); A. V. Nedospasov, V. G. Petrov, and G. N. Fidel'man, Nucl. Fusion **25**, 21 (1985).

9. F. L. Waelbroeck and R. D. Hazeltine, Bull. Am. Phys. Soc. **33**, 2012 (1988).

10. F. L. Hinton, private communication.

11. See, for example, P. H. Rutherford, Phys. Fluids **13**, 482 (1970).

12. Ch. P. Ritz, private communication.

Figure Captions

1. The solid curve is the predicted sheath potential in electron volts. The abscissa measures minor radius as a fraction of the limiter radius. The experimental points shown were measured on TEXT; one error bar, showing typical shot-to-shot variation in the $r < a$ region, is indicated.

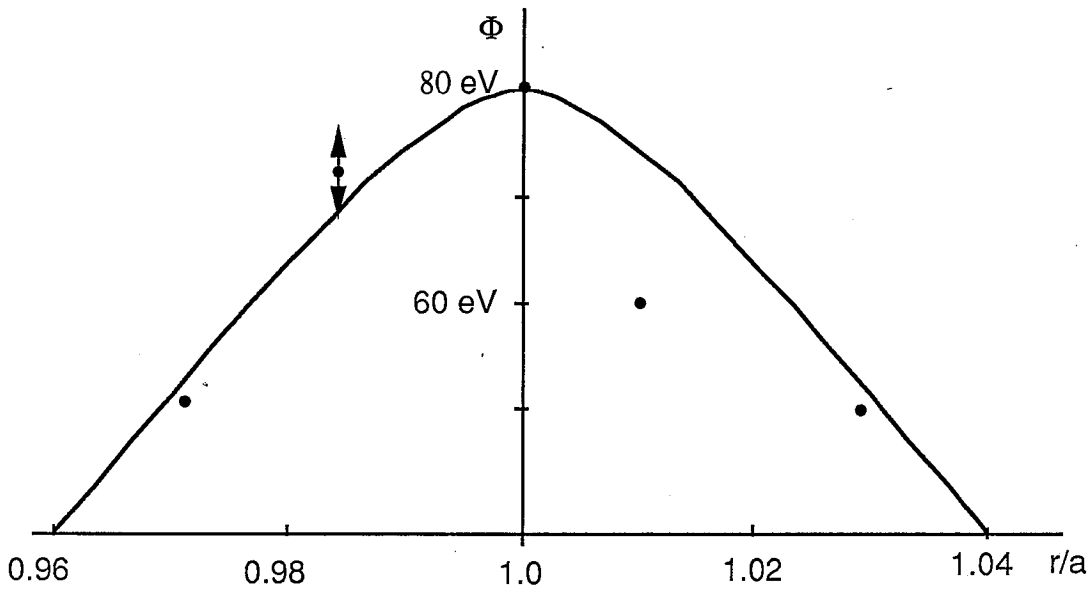

Figure 1